Electronic Supplementary Information

Commercialisation of High Energy Density Sodium-ion Batteries: Faradion's Journey and Outlook

Ashish Rudola, Anthony Rennie, Richard Heap, Seyyed Shayan Meysami, Alex Lowbridge, Francesco Mazzali, Ruth Sayers, Christopher J. Wright and Jerry Barker*

Faradion Limited, The Innovation Centre, 217 Portobello, Sheffield S1 4DP, UK

Email: jerry.barker@faradion.co.uk

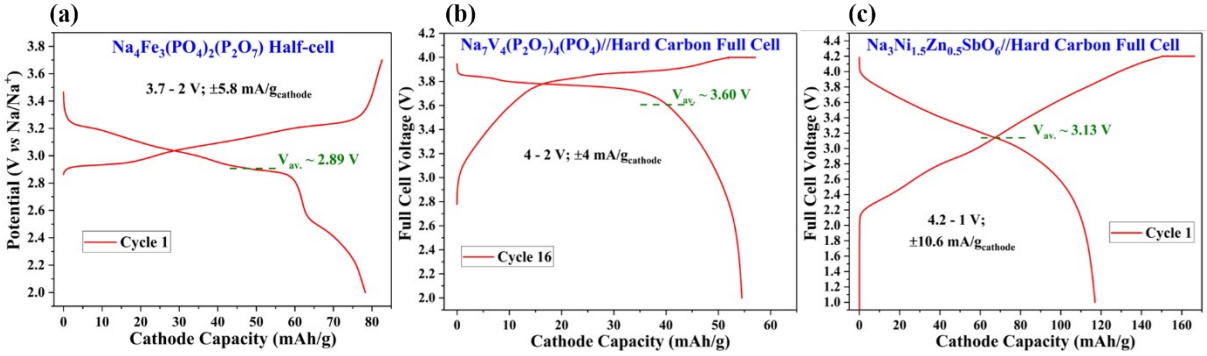

Fig. S1 Electrochemical cycling curves of some of Faradion's early cathode investigations *circa* late 2011. (a) Cycle 1 of a $Na_4Fe_3(PO_4)_2(P_2O_7)$//Na cell. (b) Cycle 16 of a $Na_7V_4(P_2O_7)_4(PO_4)$//hard carbon full cell cycled between 4 – 2 V. (c) The first cycle of a $Na_3Ni_{1.5}Zn_{0.5}SbO_6$//hard carbon full cell cycled between 4.2 – 1 V. The electrolyte used was 0.5 M $NaClO_4$ in PC.

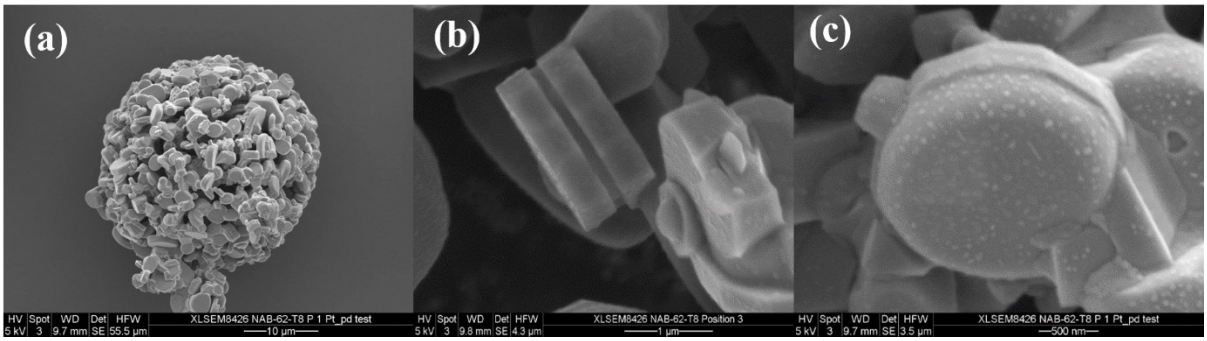

Fig. S2 FESEM images of Faradion's Gen 2 cathode material. (a) A zoomed-out image showing a ~20 µm aggregate composed of ~1 µm primary particles. (b,c) Higher magnification images clearly showing the stacked morphologies of the primary particles. The FESEM images are courtesy of Haldor-Topsøe A/S.

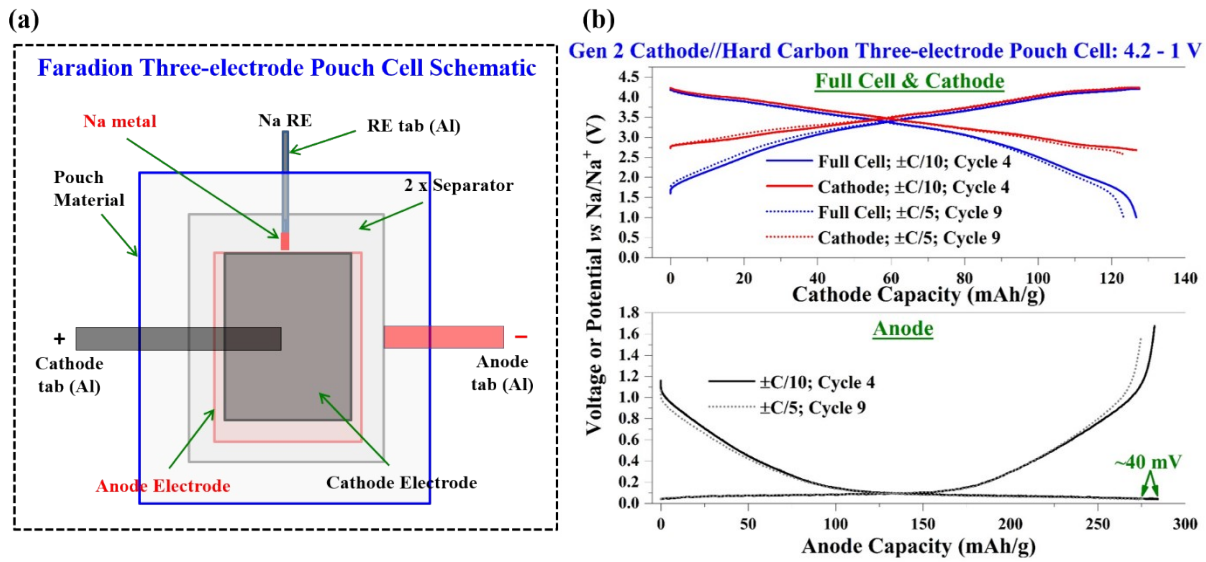

Fig. S3 Evaluation of cathode and anode potentials in the course of cycling for Faradion's Gen 2 Cathode//Hard Carbon Na-ion cells utilising three-electrode pouch cells. (a) A schematic of Faradion's in-house designed three-electrode pouch cell. The Na RE (reference electrode) is inserted in-between two layers of separators with the Na RE being as close as possible to the cathode//anode stack to ensure accurate readings. (b) Example of three-electrode cycling curves obtained at ±C/10 or ±C/5 rate when the Na-ion cell is cycled between 4.2 – 1 V. Due to higher internal resistance in three-electrode cells owing to the use of two polyolefinic separators, performance in a three-electrode cell will be inferior than in two-electrode cells especially at higher rates. As such, the hard carbon potential at 4.2 V indicated by the three-electrode cell (□40 mV) is the lower limit and likely to be higher in actual two-electrode cells. Despite this, a 40 mV value, even upon repeated cycling, is more than high enough to ensure no Na plating.

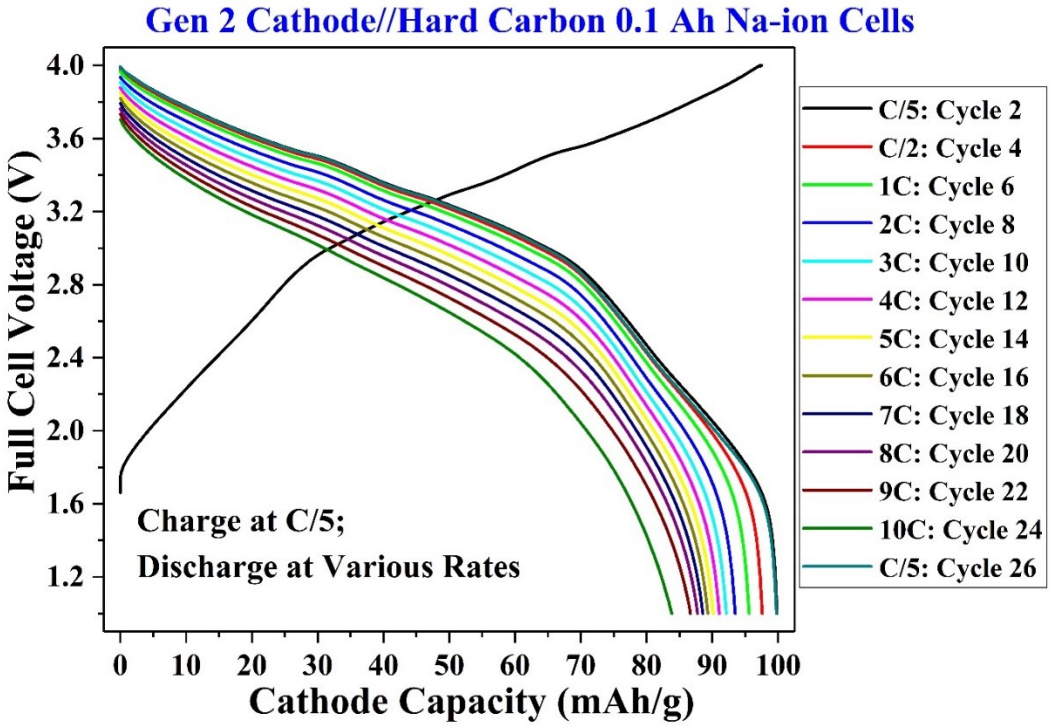

Fig. S4 Rate performance of Faradion's 0.1 Ah Na-ion pouch cells utilising its Gen 2 cathode and commercial hard carbon anode. The full cell was charged at C/5 at all rates while being discharged at various rates as indicated for two cycles each, before being cycled at ±C/5 again for the last two cycles.

Table S1 Practical specifications of some of the hard carbon precursors screened by Faradion.

#	Precursor	Formulation wt.%	Type	As-received moisture content	As-received form	Cellulose content (wt.%)	Initial drying	Initial crushing	Purification	Carbonisation	Milling	Milling energy	Pyrolysis yield (wt.%)	Total yield (wt.%)	Mass of hard carbon per £10 precursor (kg)	Tap density (g/cm^3)
1	Charcoal	100	Charred lignocellulosic	Low	Chunks	45	✓	✓	✓	✗	✓	High	80-85	80-85	6.48	0.59
2	Biochar	100	Charred lignocellulosic	33 wt.%	Small chunks	45	✗	✓	✓	✗	✓	High	72	48-49	2.03	0.59
3	Potato starch	100	Polysaccharide	Low	Fine powder	0	✗	✗	✗	✓	✓	Low	40-41	26-27	0.06	0.84
4	Rice hull	100	Lignocellulosic	Low	Small flakes	35	✗	✓	✓	✗	✓	Low	44-55	---	---	0.78
5	Olive stone	100	Lignocellulosic	Low	Fine powder	32	✗	✗	✓	✗	✓	High	32	19	1.40	0.70
6	Lignin	100	Lignin	47.5 wt.%	Powder	0	✓	✗	✓	✗	✓	Low	43-44	22-23	3.95	0.81-0.85
7	Walnut shell	100	Lignocellulosic	Low	Powder	24	✗	✗	✓	✗	✓	High	30	---	---	0.79
8	Granulated sugar	100	Disaccharide	Low	Granulates	0	✗	✗	✗	✓	✓	Low	44-50	27	3.91	0.85
12	GS/Lignin	75:25	Saccharide - Lignin	11.9 wt.%	Granulates, powder	0	✓	✗	✓	✓	✓	High	49-50	26	3.94	0.78
13	GS/Lignin	50:50	Saccharide - Lignin	23.7 wt.%	Granulates, powder	0	✓	✗	✓	✓	✓	Moderate	48	24-25	3.89	0.81
14	Anthracite*	100	Coal (92-98 wt.% C)	3.1 wt.%	Grains	0	✓	✗	?	✗	✓	Very High	90-91	87-89	28.39	1.14
15	Cellulose paper	100	Cellulose	Low	Paper	100	✗	✓	✗	✓	✓	Low	54	18	---	---
16	Microcrystalline Cellulose	100	Cellulose	Low	Fine powder	100	✗	✗	✗	✗	✓	Low	22	22	0.31	---
17	Coconut shell	100	Lignocellulosic	Low	Half shells	48	✓	✓	✓	✓	✓	Very High	93	18	0.12	0.87
18	Coconut shell charcoal	100	Charred lignocellulosic	Low	Small chips	---	✗	✓	✓	✗	✓	Very High	76.4	52-53	1.23	---
19	Douglas fir bark	100	Lignocellulosic	High	Chunks	< 20	✓	✓	✓	✓	✓	Low	94	33.3	0.44	0.89
21	Glucosamine HCL	100	Saccharide	Low	Powder	0	✗	✗	✗	✓	✓	Low	62-63	19-20	0.09	0.70
22	Pomegranate peel	100	Lignocellulosic	Low	Powder	17-22	✗	✗	✓	✓	✓	Low	89-90	17-18	0.11	---
23	Chicken manure	100	Fertiliser	32 wt.%	pellet	---	✗	✓	✓	✓	✓	Low	---	---	7.14	---

* Soft carbon

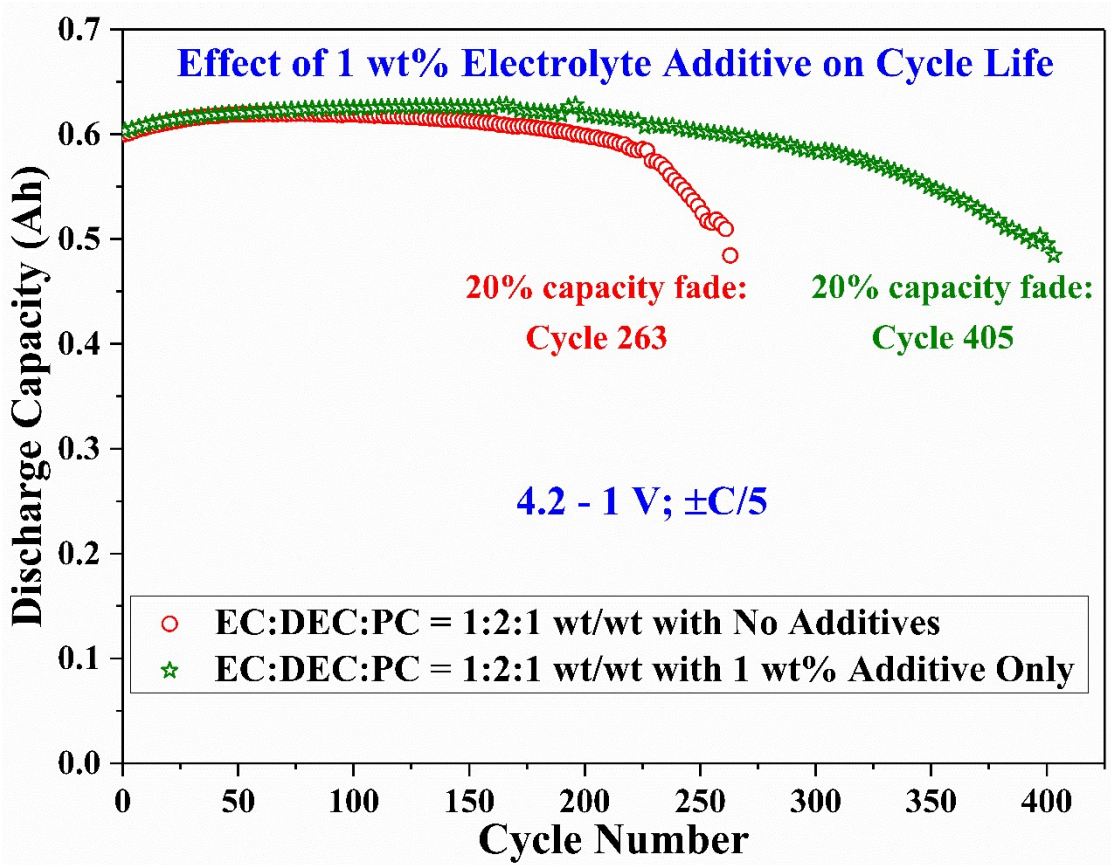

Fig. S5 Effect of 1 wt% electrolyte additive (with respect to solvent wt) in an EC:DEC:PC = 1:2:1 wt/wt based electrolyte on Faradion's old and unoptimized 0.6 Ah Na-ion pouch cells utilising its Gen 2 cathode and commercial hard carbon anode. The full cells were cycled between 4.2 – 1 V at ±C/5 at 30 °C.

Supplementary Note 1: Abuse testing on Faradion 2 Ah and 10 Ah pouch cells at the fully charged state

For the abuse testing, 10 Ah and 2 Ah pouch cells were fabricated within projects part funded by Innovate UK, the UK's innovation agency. These 2 and 10 Ah pouch cells were tested by Warwick Manufacturing Group, following test protocols defined in *IEC 62660-2 - Secondary lithium-ion cells for the propulsion of electric road vehicles - Part 2: Reliability and abuse testing*. Prior to the abuse testing, the cells were formed, degassed and cycled 20 times. Details on each test are mentioned below.

External Short Circuit Test: For the external short test, the state of charge (SOC) of the pouch cell was adjusted to 100 % SOC (full cell voltage of 4.2 V) and then, the terminals of the pouch cell were connected to each other using a low-resistance connection to effectively short-circuit the cell for 10 minutes. This resulted in a minor expansion of the pouch cell and the cell temperature rose to a maximum of 96 °C. However, no violent reaction was observed and the subsequent contraction of the pouch suggested that the expansion was largely caused by heating rather than decomposition of the cell components leading to gassing.

Overcharge Test: The overcharge test involved adjusting the pouch cell to 100 % SOC and this was followed by further charging at a 1 C rate. No violent reaction was observed and the maximum temperature of the pouch cell reached just 24 °C. This test was stopped when the cell capacity reached the pass criterion of twice its rated capacity.

Hot Box Test: The high temperature endurance test, commonly known as a hot box test, involved adjusting the SOC of the cell to 100 %, before placing it in an oven and raising the temperature at 5 °C/minute to 130 °C. This temperature was then maintained for a period of 30 minutes. During this time, a minor voltage drop was observed temporarily and no violent reaction occurred.

Crush Tests: Crush tests were performed in two ways, by applying force from a different direction in each case. During the flat crush test, the cell was adjusted to 100 % SOC and laid on a flat surface, face-up. A crushing force was then applied, using a round crushing tool, until a force of 1000 times the weight of the cell was achieved. During the edge-on crush test, the cell was adjusted to 100 % SOC and the cell was then placed on its side between two plates. A crushing force was then applied to the edge of the cell, using a bar-shaped crushing tool, until the cell deformed by > 15 % of its original width. In both cases, no violent reaction occurred and there were negligible changes in temperature or voltage.

Nail Penetration Test: For this test, the cell was adjusted to 100 % SOC and then a 3 mm diameter steel nail was made to drive through the cell. This nail was held in place until the cell temperature returned to ambient. No violent reaction was observed, and the maximum temperature reached was just 41 °C. Note: this test is not part of the IEC 62660-2 test protocol; however, we included this popular abuse test as passing this test successfully is important from a safety point of view.

In summary, the abuse testing results on Faradion's first generation product pouch cells have been very positive, indicating the excellent safety characteristics of this Na-ion technology.

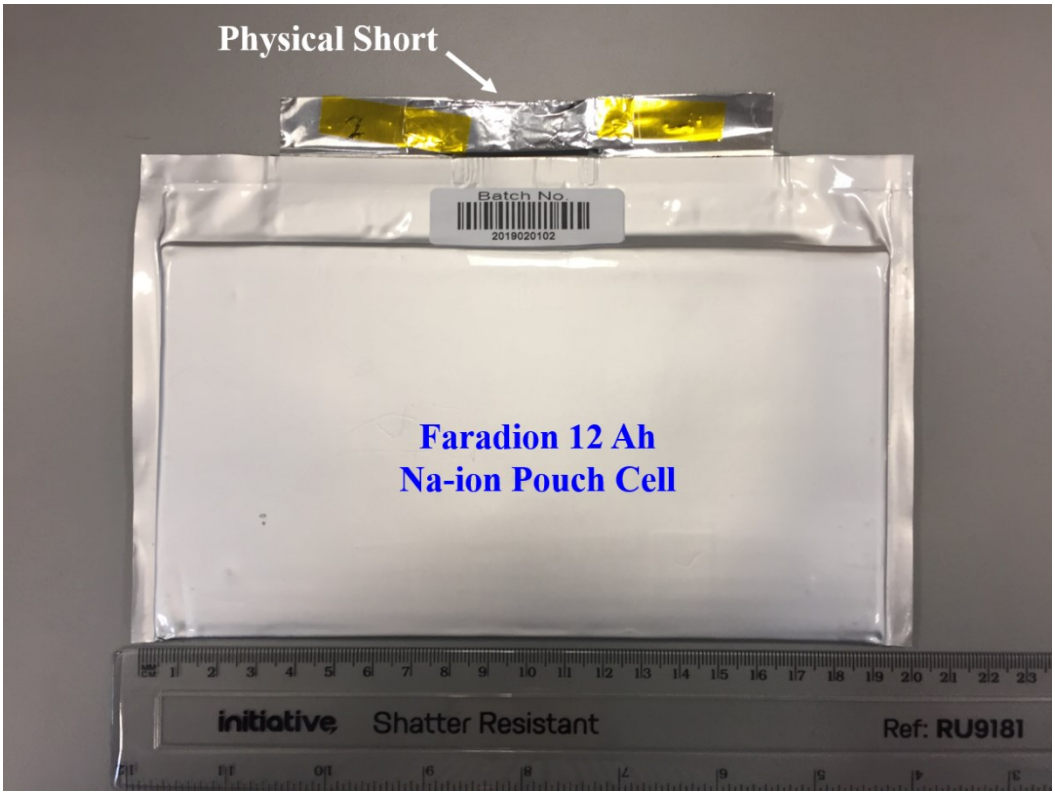

Fig. S6 An example of how Faradion stores and ships its commercial Na-ion pouch cells. The figure above showcases a 12 Ah pouch cell manufactured by one of Faradion's commercial partners, which was shipped and then received at Faradion in the shorted state, with a shunt connected between the cathode and anode terminals to cause a physical short.

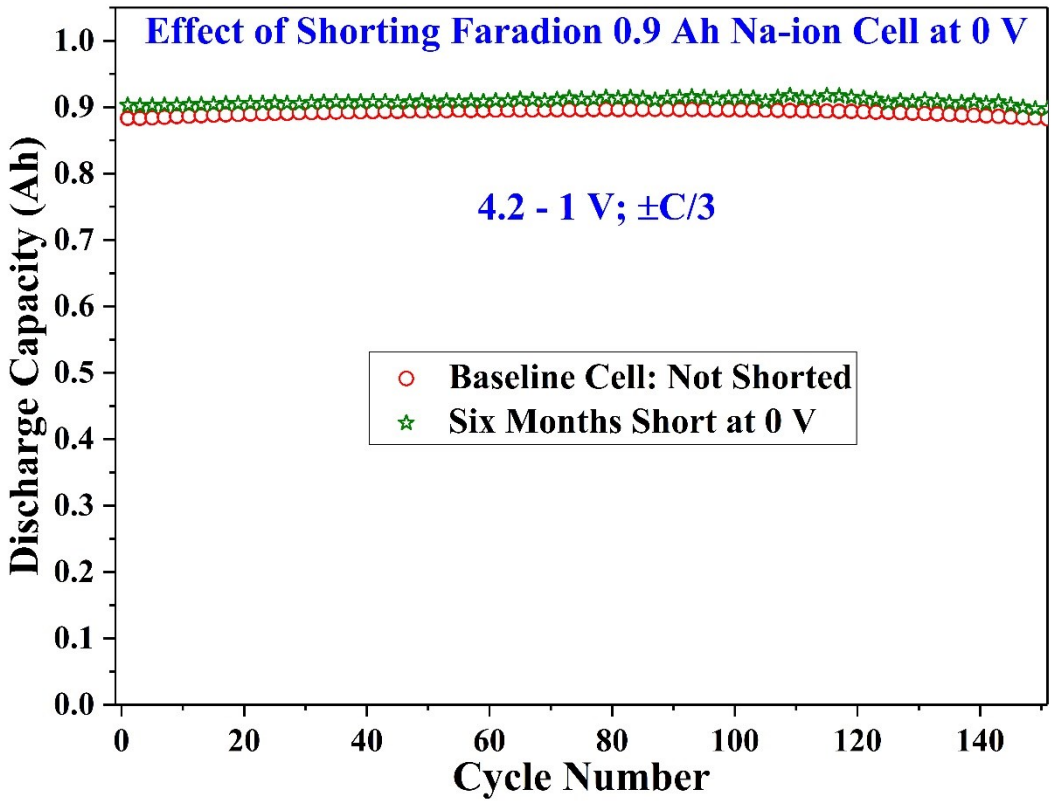

Fig. S7 Long-term cycling of Faradion Na-ion 0.9 Ah pouch cells with one pouch cell having been kept at 0 V for six months in ambient environment (~19 °C) after formation cycling, while the other cell having been cycled as normal after formation cycling (without shorting at 0 V). An actual low resistor shunt was connected between the cathode and anode terminals for the shorted cell during the six-month storage at 0 V.

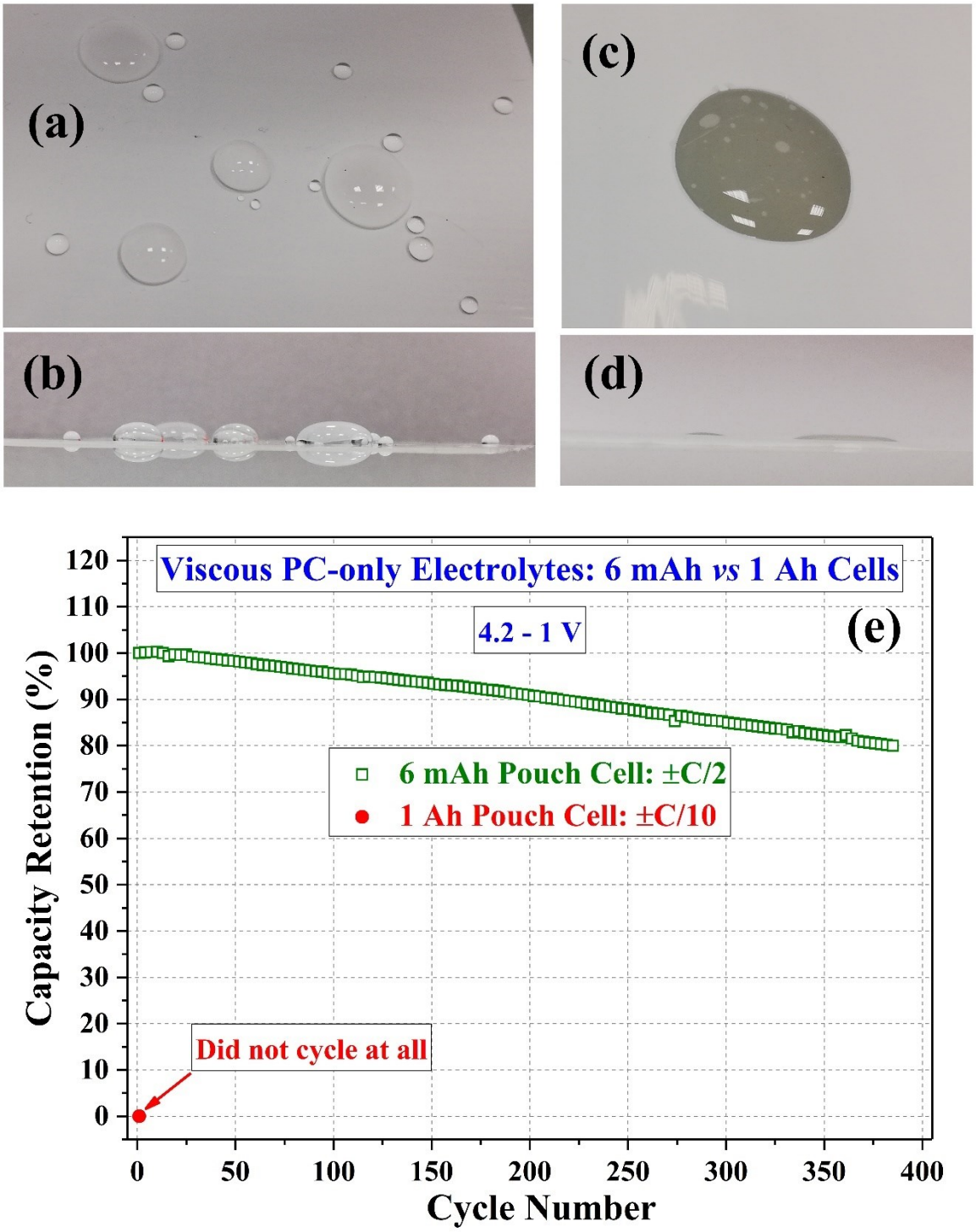

Fig. S8 (a-d) Electrolyte wetting results on commercial polyolefinic Celgard 2500 separators using (a, b) 17 m $NaClO_4$ in water water-in-salt concentrated electrolyte and (c, d) PC-dominant electrolyte with PC wt % > 75 % in the solvent blend. For both electrolytes, images are shown from the top (a, c) and perpendicularly side-on (b, d) with respect to the separator. Both sets of experiments were identical, with the only difference being the electrolyte used. It can clearly be seen that the water-in-salt concentrated electrolyte does not wet the separator to any practically relevant degree, while a PC-dominant electrolyte can satisfactorily wet the commercial separator. (e) Effect of cell size in scaling-up viscous PC-only electrolytes. When using $NaPF_6$ in just PC solvent as the electrolyte (with non-diluting additives), the performance obtained in experimental 6 mAh Na-ion pouch cells is satisfactory: 385 cycles to 20% capacity fade at ±C/2 rate. However, when this cell design was scaled to 1 Ah Na-ion pouch cells, the cell did not even cycle at ±C/10 during the formation cycles.

Supplementary Note 2: Closed-cup flash point testing of various Na-ion liquid electrolytes

Table S2 lists the closed-cup flash point testing results on various liquid electrolytes along with the type of closed-up testing method used for each sample.

Method: For each sample, ~200 – 250 ml was supplied to an external contractor and results from 2-3 runs for each sample were used to accurately estimate the flash point. The closed-cup method used has been indicated for each sample, as indicated. The Abel closed-cup method is suitable to a temperature of 70 °C; for more thermally stable liquids demonstrating a flash point > 40 °C, the Pensky Marten method should be used.[1] For samples with no flash point detected below 120 °C, the experiment was ceased at 120 °C by the contractor due to excessive black smoke, indicating decomposition of the electrolyte without reaching a flash point.

Discussion: An example of a widely used commercial electrolyte, LP 30, has been included here as well, demonstrating its low flash point and highly flammable nature. A popular fire-retardant solvent, trimethyl phosphate (TMP), can raise an electrolyte's flash point, but the inclusion of flammable co-solvents places a limit to the extent of the increase in the flash point, consistent with the observations of Hess *et al.*. However, inclusion of TMP would certainly decrease the electrolyte blend's resultant self-extinguishing time (SET) to the point of non-flammability, despite a relatively lower flash point, a behaviour we observed as well in our SET experiments (not shown here).[1] For the PC-based electrolytes, two different diluents (A and B) were investigated and both resulted in non-flammable electrolyte blends (TEL 43e and TEL 58a are identical apart from the type of diluent used). The flash point testing results of these PC-majority electrolyte blends conclusively indicate that such electrolytes would likely not catch fire even under abuse conditions, alleviating fears of thermal runaway leading to fires/explosions of Faradion's Na-ion batteries using such electrolytes.

Table S2 Closed-cup flash point testing results on various Na-ion liquid electrolytes.

#	Sample	Description	Flash Point Testing Results	Method
1	LP 30	1 M $LiPF_6$ in EC:DMC = 1:1 v/v	32.0 °C	IP 170 (Abel closed-cup)
2	TEL 0	$NaPF_6$ in EC:DEC:PC = 1:2:1 wt/wt	38.5 °C	IP 170 (Abel closed-cup)
3	TEL 0+ (131)	$NaPF_6$ in EC:DEC:PC = 1:3:1 wt/wt	37 °C	IP 170 (Abel closed-cup)
4	151	$NaPF_6$ in EC:EMC:PC = 1:5:1 wt/wt	26.5 °C	IP 170 (Abel closed-cup)
3	TEL 14d	$NaBF_4$ in (EC:DEC:PC = 1:2:1 wt/wt):TMP = 1:1 wt/wt with 2 wt% additives	44 °C	IP 170 (Abel closed-cup)
4	TEL 24b	$NaPF_6$ in EC:DEC:PC = 1:2:1 wt/wt with 2 wt% additives	38.5 °C	IP 170 (Abel closed-cup)
5	TEL 43c	$NaPF_6$ in PC with 40wt% diluent A and 3 wt% additives	No flash point detected till 120 °C; sample emitted black smoke from 90 °C	IP 34 (Pensky Marten closed-cup)
6	TEL 43e	$NaPF_6$ in PC with 20wt% diluent A and 3 wt% additives	No flash point detected till 120 °C; sample emitted black smoke from 90 °C	IP 34 (Pensky Marten closed-cup)
7	TEL 49d	$NaBF_4$ in PC:TMP = 1:1 wt/wt with 20 wt% diluent	No flash point detected till 120 °C; sample emitted black	IP 34 (Pensky Marten

		A and 4wt% additives	smoke from 90 °C	closed-cup)
8	**TEL 58a**	$NaPF_6$ in PC with 20 wt% diluent B and 3 wt% additives	No flash point detected till 120 °C; sample emitted black smoke from 90 °C	IP 34 (Pensky Marten closed-cup)

Supplementary Note 3: Voltammetry loop investigations on oxidative stabilities of PC-dominant Na-ion electrolytes

Method: We quantitatively investigated the oxidative stability of three Na-ion electrolytes through Linear Sweep Voltammetry (LSV) loops. In these LSV experiments, three-electrode pouch cells were fabricated with the cathode and anode consisting of just pure Al current collector foils. In these LSV experiments, the filled three-electrode cells were cycled at a slow 2 mV/s scan rate to 3.8 V *vs* Na/Na^+ (based on the Na reference electrode), cycled back down to 2.5 V and then cycled again to the next upper cut-off potential. This process was repeated with the following cut-off potentials: 3.8 V, 4.2 V, 4.4 V, 5 V and finally to 8 V. Such an experiment, which can be regarded as a cross between a cyclic voltammetry and LSV experiment, is advantageous in providing accurate values of charge passed at any potential band (such as 4.4 – 5 V *vs* Na/Na^+). It should be noted that such types of experiments are heavily influenced by the scan rate of the experiment – faster scan rates such as 10 mV/s (used quite frequently in the literature) tend to underestimate degree of electrolyte oxidation due to kinetic (polarisation) effects. This is why a slow value of 2 mV/s was chosen in this experiment to avoid such complications.

Since these three-electrode cells contain no active materials on the cathode/anode, it is thought that the magnitude of charge passed provides an indication to the extent of electrolyte oxidation on the Al current collectors: the lower the charge consumed, the less the electrolyte would be prone to oxidation and hence, the better the electrolyte's performance will be when used in actual Na-ion cells and charged to voltages of similar magnitude. Of course, it is known that the conductive carbon and/or the cathode active material present in actual full cells can act as catalysts for the electrolyte oxidation reactions at such high potentials. Keeping in mind that such possible catalytic effects might be transpiring in actual full cells, we chose to use very high upper cut-off potentials, such as 5 V or 8 V *vs* Na/Na^+: such high potential values might serve as a substitute for such catalysing effects, which will not occur in these three-electrode cells using Al current collectors and, as such, might provide a more representative picture of the level of electrolyte oxidation experienced in actual full cells.

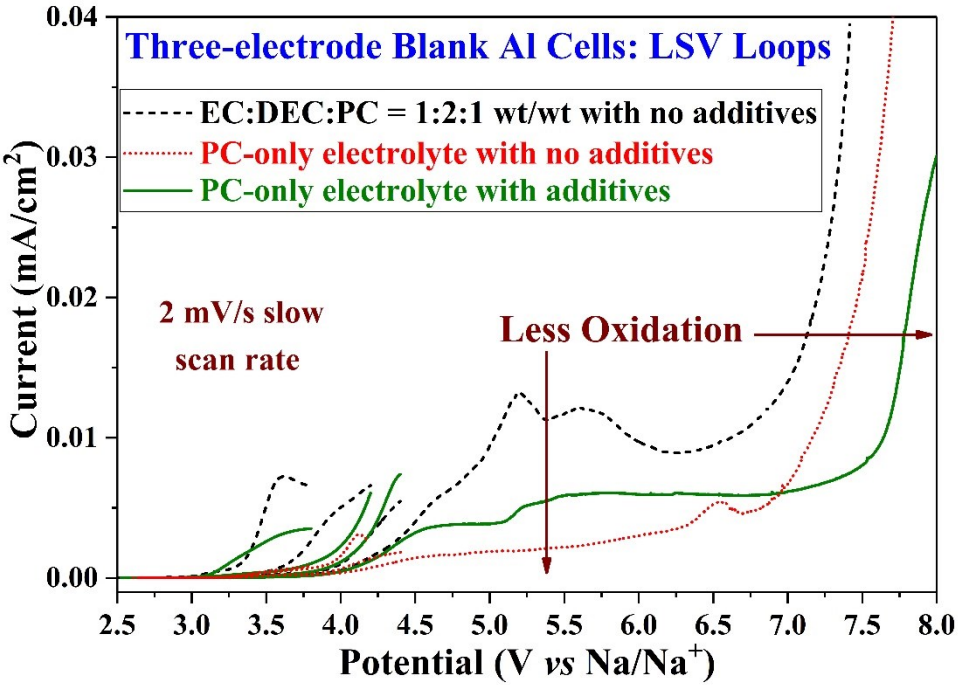

Fig. S9 LSV Loop investigations on three-electrode pouch cells based on bare Al cathodes and anodes filled with PC-only or EC:DEC:PC = 1:2:1 electrolytes. The salt used here is $NaPF_6$ at the same concentration.

Results: Fig. S9 presents the actual current-voltage curves obtained: as indicated by the arrows, the lower the current at a particular voltage value, and the higher the voltage value before complete electrolyte breakdown (indicated by the exponential increase in current above 7 V), the less susceptible the electrolyte should be to oxidation in actual Na-ion cells. From Fig. S9, it is qualitatively apparent that the two PC-based electrolytes demonstrated a much lower charge current at various potential bands, along with higher onset of complete electrolyte breakdown with respect to the baseline electrolyte, based on a EC:DEC:PC solvent blend.

Table S3 Magnitude of charge passed at various potential bands investigated in the LSV loop experiments. Values in parentheses indicate the relative differences in magnitude of Electrolytes 2 and 3 *vs* Electrolyte 1.

#	Electrolyte	Q(mC): 3.8 – 4.2 V (% wrt Case 1)	Q (mC): 4.2 – 4.4 V (% wrt Case 1)	Q (mC): 4.4 – 5 V (% wrt Case 1)	Q (mC): 5 – 8 V (% wrt Case 1)	Total Q (mC): 3.8 – 8 V (% wrt Case 1)
1	$NaPF_6$ in EC:DEC:PC = 1:2:1 wt/wt	1.06	0.43	2.79	150.78	155.05
2	$NaPF_6$ in PC	0.39 **(-63.4 %)**	0.22 **(-49.2 %)**	1.07 **(-61.4 %)**	69.67 **(-53.8%)**	71.35 **(-54 %)**
3	$NaPF_6$ in PC with additives	0.55 **(-48 %)**	0.45 **(+4.2 %)**	1.99 **(-28.6 %)**	51.23 **(-66 %)**	54.21 **(-65 %)**

Table S3 above provides quantitative values of the charge passed (in units of mC) by the respective electrolyte solutions in the various potential bands studied. All three electrolytes studied contained the same concentration of $NaPF_6$ salt. From Table S3, it becomes clear that Electrolyte 2 (PC as the sole solvent) demonstrated much lower charge passed at each potential band, particularly the two higher potential bands of 4.4 – 5 V and 5 – 8 V. In fact, the irreversible charge consumed due to electrolyte oxidation for Electrolyte 2 was 54% lower than Electrolyte 1 over the total 3.8 – 8 V range studied in this experiment.

Electrolyte 3, which is also PC-based, included targeted electrolyte additives to serve various functions, one of them being to ensure excellent high voltage performance. The impact of the additives is obvious from this table: Electrolyte 3 demonstrated the lowest total irreversible charge consumed over the entire 3.8 – 8 V range out of all three electrolytes studied and was 65% lower than Electrolyte 1.

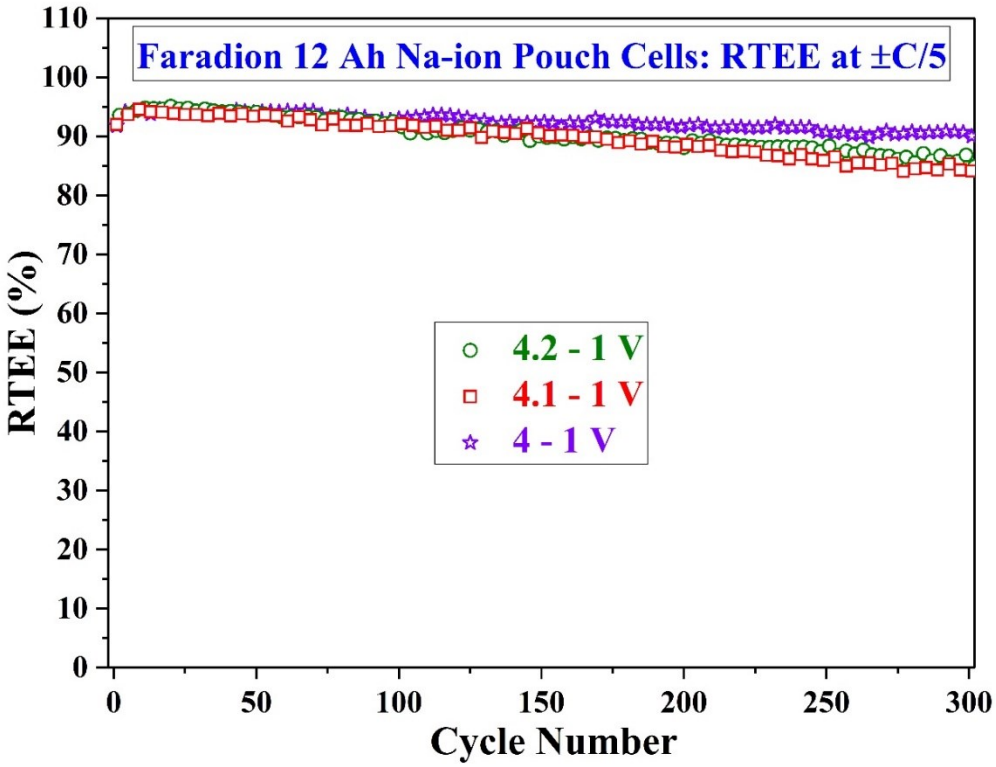

Fig. S10 Round-Trip-Energy-Efficiency (RTEE) of Faradion's 12 Ah Na-ion pouch cells at ±C/5 at three different voltage windows. RTEE values of ~94-95 % were obtained, indicating the excellent efficiency of Faradion's first generation Na-ion production-category pouch cells.

Table S4 Comparison of Na-ion full cells reported in the literature with capacity exceeding 50 mAh

#	Cell Type	Cathode	Anode	Electrolyte	ED (Wh/kg)	Av. Disch. V (V)	Cycling Stability	V Window	Ref.
18650 Cells									
1	18650 (~570 mAh)	$Na_3V_2(PO_4)_2F_3$	Hard Carbon	1 M $NaPF_6$ in EC:PC + 0.5% NaODFB + 3% PS + 1% SN + 3% VC	-	~3.6 at **55 °C**	-	4.25 – 2 V	[2]
2	18650 (430 mAh)	R-$Na_2Fe_2(CN)_6$	Hard Carbon	1 M $NaBF_4$ in Tetraglyme	43	3.0	100% capacity, 93% energy retention in 100 cycles at ±C/5	3.4 – 1 V	[3]
3	18650 (560 mAh)	$Na_{3.2}V_{1.8}Zn_{0.2}(PO_4)_3$	Hard Carbon	1 M $NaBF_4$ in Tetraglyme	60	3.25	90% capacity retention in 200 cycles at ±C/5	4.1 – 1 V	[4]
4	18650	O3-$Na_{0.9}Cu_{0.12}Ni_{0.10}Fe_{0.30}Mn_{0.43}Ti_{0.05}O_2$	Hard Carbon	1 M $NaBF_4$ in Tetraglyme	62	3.0	87% capacity retention in 80 cycles at ±C/5	4.1 – 1 V	[5]
5	18650	$Na_3V_2(PO_4)_2F_3$	Hard Carbon	1 M $NaPF_6$ in EC:DMC	75	3.4	80% capacity retention in 3750 cycles at ±1 C	4.25 – 2 V	[6]
6	18650 (~1 Ah)	O3-$NaNi_{0.45}Zn_{0.05}Mn_{0.4}Ti_{0.1}O_2$	Hard Carbon	1 M $NaPF_6$ in EC:DMC	~97	~2.85	-	4.4 – 1.2 V	[7]
Pouch Cells									
1	880 mAh Pouch Cell	$NaNi_{1/3}Fe_{1/3}Mn_{1/3}O_2$	Hard Carbon	0.8 M $NaPF_6$ in PC:EMC with additives	-	~2.75	80% capacity retention in 2500 cycles at ±1 C	3.8 – 1.5 V	[8]
2	880 mAh Pouch Cell	$NaNi_{1/3}Fe_{1/3}Mn_{1/3}O_2$	Hard Carbon	1.5 M $NaPF_6$ in F-EPE:TMP = 1:2 v/v with 2 wt% FEC	-	~2.9	70.8% capacity retention in 500 cycles at ±1 C	3.8 – 1.5 V	[9]
3	5 Ah Pouch Cell	$Na_{2-x}Fe_2(CN)_6$	Hard Carbon	1 M $NaPF_6$ in EC:DEC = 1:1 v/v with 2 vol% FEC	-	~2.6	78% capacity retention in 1000 cycles at ±1 C	3.2 – 1 V	[10]
4	1 Ah Pouch Cell	$NaNi_{1/3}Fe_{1/3}Mn_{1/3}O_2$	Hard Carbon	1 M $NaPF_6$ in PC:EMC = 1:1 v/v with 2 wt% FEC	95	~2.95	92.6% capacity retention in 100 cycles at ±1 C	3.8 – 2 V	[11]
5	110 mAh Pouch Cell	O3-$NaNi_{0.5}Mn_{0.3}Co_{0.2}O_2$	Hard Carbon	1 M $NaClO_4$ in EC:DEC	100	~2.9	~50% capacity retention in 70 cycles at ±C/5	4 – 1.5 V	[12]
6	2 Ah	O3-	Anthraci	0.8 M $NaPF_6$	100	3.2	~94%	4 – 1.5 V	[13]

	Pouch Cell	$Na_{0.9}[Cu_{0.22}Fe_{0.30}Mn_{0.48}]O_2$	te Hard Carbon	in PC:EMC with additives			capacity retention in 50 cycles at ±C/10		
7	0.5 - 5 Ah Pouch Cell	$Na_xMnFe(CN)_6$	Hard Carbon	-	100 – 130	3.2	98.6% capacity retention in 500 cycles at ±1 C	4 – 1.5 V	[14]
8	Pouch Cell	O3- Na_x[Li-Cu-Fe-Mn]O_2	Amorphous Hard Carbon	-	135	~2.83	91% capacity retention in 1000 cycles at ±3 C	4 – 1.5 V	[15]
9	12 Ah Pouch Cell	Gen 2 Cathode	Hard Carbon	$NaPF_6$ in EC:DEC:PC = 1:2:1 wt/wt with additives	160	3.2	80% capacity retention in > 3,000 cycles at ±1 C at 4 – 1 V	4.2 – 1 V	Far 2020
Prismatic Cell									
1	27 Ah Prismatic Cell	O3-$NaCrO_2$	Hard Carbon	Na[FSA]–[C_3C_1pyrr][FSA] = 20:80 mol% ionic liquid	75	~2.7	87% capacity retention in 500 cycles at ±C/2.7 at **60 °C**	3.35 – 1.5 V	[16]

Note: In compiling this list, we didn't include any full cells that used pre-sodiation/pre-cycling techniques to deal with irreversible capacities of the anode or cathode, as such methods are currently not commercially feasible and it would take significant efforts to make it so.

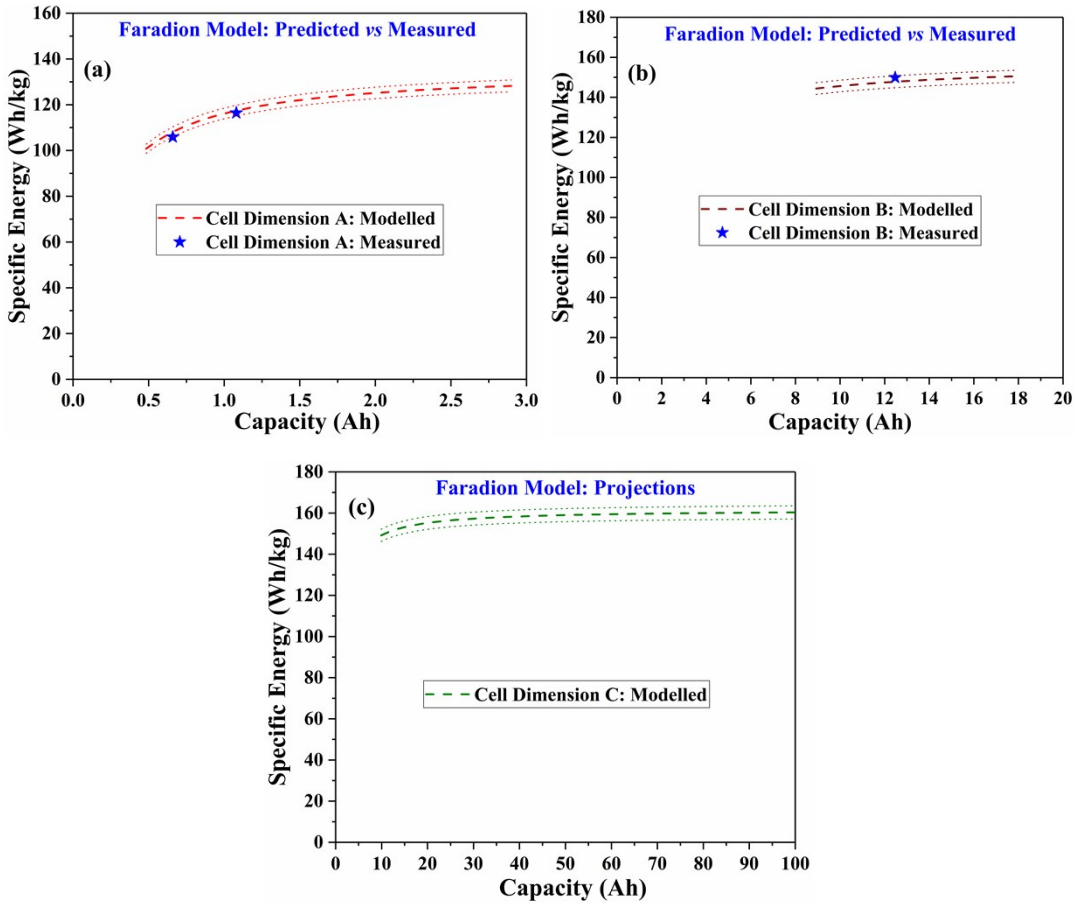

Fig. S11 Illustrations showing the accuracy of Faradion's Na-ion modelling capabilities across various cell dimensions corresponding to different pouch cell capacities. For Na-ion pouch cells with (a) Dimension A (corresponding to cell capacities under 3 Ah) and (b) Dimension B (corresponding to cell capacities around 8 – 18 Ah), the predicted specific energy values (dashed lines) match those of the measured values determined experimentally (solid points), within ±2 % (the dotted lines). (c) Using Faradion's model, the projected specific energies using cell Dimension C (for larger-scale pouch cells with higher capacities) indicate ~160 Wh/kg is achievable in 32 Ah pouch cells using Faradion's Na-ion chemistry; confirmation is underway.

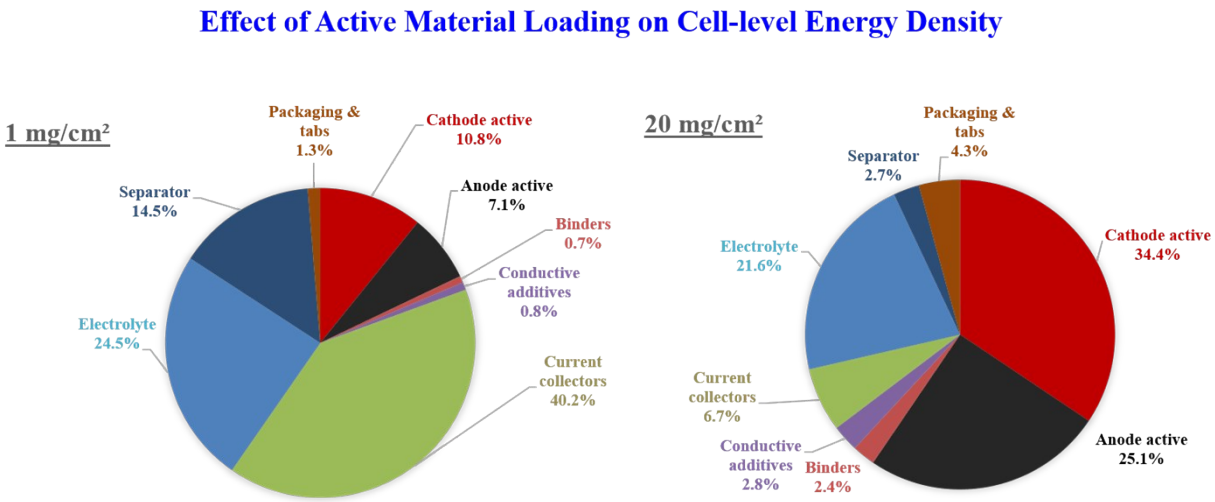

Fig. S12 Illustration of how the loading of active materials in an alkali-ion pouch cell affects the relative proportions between the electroactive components (active materials) and electrochemically inactive components in a cell. Two cases are shown: one with cathode loading of just 1 mg/cm^2 (often used in academic reports) and a much higher cathode loading of 20 mg/cm^2 (a value which could be used in typical commercial-scale cells). The anode loading is appropriately adjusted to keep the same cell balance.

Supplementary Note 4: Cost comparisons between LFP//Graphite Li-ion and Faradion's Na-ion pouch cells

Fig S13 shows a comparison of a commercial LFP//Graphite cell and Faradion's Na-ion cell based on our Gen 2 cathode//commercial hard carbon anode. The cell material cost is broken down by cell component, and modelled using BatPac v3, using today's commercial values for all cell components and, the inputs use material physical properties and electrochemical performance of Faradion's Na-ion cells.

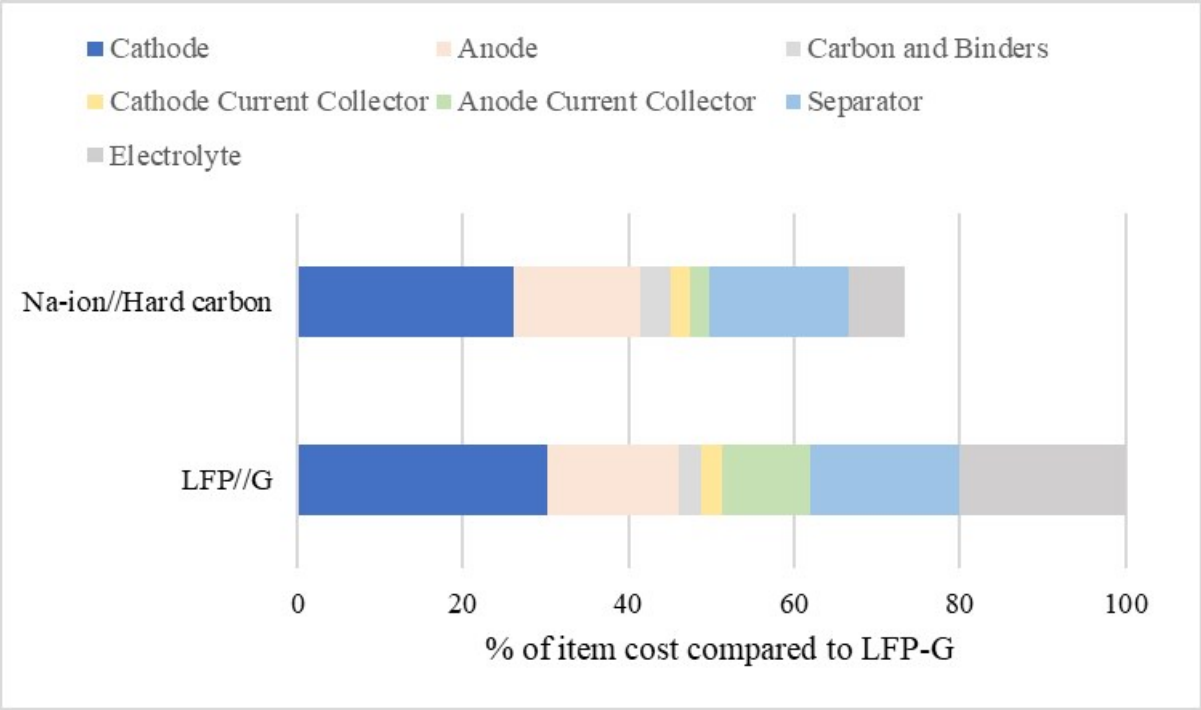

Fig. S13 Cost comparisons of LFP//Graphite Li-ion pouch cells with that of Faradion's Na-ion pouch cells. The costs have been normalised with respect to those of the LFP//Graphite system.

References

1. S. Hess, M. Wohlfahrt-Mehrens and M. Wachtler, *Journal of The Electrochemical Society*, 2015, **162**, A3084-A3097.
2. G. Yan, K. Reeves, D. Foix, Z. Li, C. Cometto, S. Mariyappan, M. Salanne and J.-M. Tarascon, *Advanced Energy Materials*, 2019, **9**, 1901431.
3. L. U. Subasinghe, G. S. Reddy, A. Rudola and P. Balaya, *Journal of the Electrochemical Society*, 2020, **167**, 110504.
4. K. Du, C. Wang, L. U. Subasinghe, S. R. Gajella, M. Law, A. Rudola and P. Balaya, *Energy Storage Materials*, 2020, **29**, 287-299.
5. A. Tripathi, A. Rudola, S. R. Gajjela, S. Xi and P. Balaya, *Journal of Materials Chemistry A*, 2019, **7**, 25944-25960.
6. T. Broux, F. Fauth, N. Hall, Y. Chatillon, M. Bianchini, T. Bamine, J.-B. Leriche, E. Suard, D. Carlier, Y. Reynier, L. Simonin, C. Masquelier and L. Croguennec, *Small Methods*, 2019, **3**, 1800215.
7. S. Mariyappan, T. Marchandier, F. Rabuel, A. Iadecola, G. Rousse, A. V. Morozov, A. M. Abakumov and J.-M. Tarascon, *Chemistry of Materials*, 2020, **32**, 1657-1666.
8. H. Che, X. Yang, Y. Yu, C. Pan, H. Wang, Y. Deng, L. Li and Z.-F. Ma, *Green Energy & Environment*, 2020.
9. Y. Yu, H. Che, X. Yang, Y. Deng, L. Li and Z.-F. Ma, *Electrochemistry Communications*, 2020, **110**, 106635.
10. W. Wang, Y. Gang, Z. Hu, Z. Yan, W. Li, Y. Li, Q.-F. Gu, Z. Wang, S.-L. Chou, H.-K. Liu and S.-X. Dou, *Nature Communications*, 2020, **11**, 980.
11. Y. Xie, G.-L. Xu, H. Che, H. Wang, K. Yang, X. Yang, F. Guo, Y. Ren, Z. Chen, K. Amine and Z.-F. Ma, *Chemistry of Materials*, 2018, **30**, 4909-4918.
12. V. K. Kumar, S. Ghosh, S. Biswas and S. K. Martha, *Journal of The Electrochemical Society*, 2020, **167**, 080531.
13. Y. Li, Y.-S. Hu, X. Qi, X. Rong, H. Li, X. Huang and L. Chen, *Energy Storage Materials*, 2016, **5**, 191-197.
14. A. Bauer, J. Song, S. Vail, W. Pan, J. Barker and Y. Lu, *Advanced Energy Materials*, 2018, **8**, 1702869.
15. X. Rong, Y. Lu, X. Qi, Q. Zhou, W. Kong, K. Tang, L. Chen and Y. Hu, *Energy Storage Science and Technology*, 2020, **9**, 515-522.
16. A. Fukunaga, T. Nohira, R. Hagiwara, K. Numata, E. Itani, S. Sakai and K. Nitta, *Journal of Applied Electrochemistry*, 2016, **46**, 487-496.